



Adsorption of Heavy Metals from Contaminated Water using Leachate Modular Tower

Frank Aneke^{1*}, Joy Adu²

¹ *Geotechnics and Materials Development Research Group (GMDRg) Civil Engineering, University of KwaZulu-Natal, 4001, South Africa.*

² *Department of Civil Engineering, University of KwaZulu-Natal, KwaZulu-Natal, South Africa.*

Received 11 February 2023; Revised 04 May 2023; Accepted 09 May 2023; Published 01 June 2023

Abstract

The heavy metals (HMs) and metalloids such as Cr(VI), As(III), and Pb(II) in contaminated water are toxic even at trace levels and have caused devastating negative health impacts on human beings. Hence, the effective adsorption of these heavy metals from contaminated water is important to protect biodiversity, hydrosphere ecosystems, and human beings. In this study, a leachate modular tower (LMT) was developed for the singular purpose of adsorbing HMs. The LMT contained nano-slag as a liner, which was synthesized from slag. The nano-slag was blended in different proportions of 90:10; 80:20; 70:30; 60:40, and 50:50 to the combined mass of clay and nano-slag, to evaluate the most efficient ratio of the blends capable of adsorbing HMs and metalloids with 100% efficiency. A series of leachate tests were performed to evaluate the adsorption capacity of LMT with different embedded liners. Attenuation periods of 2, 5, 7, and 10 days with a temperature of 500 °C were also selected to improve the sorption rate and uptake of HMs. Subsequently, the effluents were subjected to inductive coupled plasma mass spectrometry (ICP-MS) tests to evaluate the concentrations and percentages of adsorbed HMs, which were calculated using a pseudo-first-order adsorption model. The results revealed that the removal of 98% As, 99% Cd, and 99.9% Pb was achieved with a 50%:50% ratio of soil and nano-slag as the liner at 10 days equilibrium period. Furthermore, 98% Zn, 95.45% Cu, 93.3% Fe, 97% Ni, and 89% Hg were achieved upon further investigation using the same dosage of soil and nano-slag and equilibrium conditions. The scanning electron microscopy (SEM) tests demonstrated that some traces of the absorbed HMs and metalloids were found on the liner surfaces, indicating significant changes in microstructure. The results indicated the sorption rate increased significantly due to the elevated temperature, aluminosilicate structure, and prolonged attenuation period, which are also associated with an elevated pH level and higher cation exchange capacity (CEC), of the liner.

Keywords: Contaminated Water; NSCL; Heavy Metals; LMT; Equilibrium Period.

1. Introduction

Water is one of the most valuable natural resources on earth because of its essentiality to humans, animals, plants, etc. The low standard of quality of water supplies to end-users has been on the rise in the recent past due to rapid urbanization, mining, and industrial activities. Also, the uncontrolled discharge of untreated industrial wastewater has caused serious environmental and health damage, including heavy metal pollution. Heavy metal ions refer to the metalloids that have an atomic weight in the range between 63.5 g/mol and 200.6 g/mol and a specific gravity of more than 5.0 g/cm³ [1].

This water contamination can occur through natural or anthropogenic processes, either from single or multiple sources with high toxicity. The World Health Organization, according to their report, quantified the following metalloids

* Corresponding author: anekef@ukzn.ac.za



<http://dx.doi.org/10.28991/CEJ-2023-09-06-017>



© 2023 by the authors. Licensee C.E.J, Tehran, Iran. This article is an open access article distributed under the terms and conditions of the Creative Commons Attribution (CC-BY) license (<http://creativecommons.org/licenses/by/4.0/>).

arsenic (As), copper (Cu), mercury (Hg), nickel (Ni), cadmium (Cd), lead (Pb), and chromium (Cr) as the most toxic [2]. The most common anthropogenic water contamination results from Industrial processes such as metal plating, fertilizer manufacture, petrochemical, paper making, and mining operations. This process has significantly increased the mobilization of HM to both ground and surface water sources. The aforementioned water contamination process has become a serious threat to plants, animals, and humans due to the non-biodegradable, bioaccumulation, and toxic properties of heavy metals, even at low concentrations. Therefore, the effective removal of heavy metals from aqueous solutions is crucial to protecting humans and environmental health. Bind et al. [3] suggested that long-term exposure to HMs in the environment could accumulate in the food chain and mobilize food poison due to their non-biodegradability. And could even lead to water scarcity [4, 5]. Given the prevention and control of heavy metal pollution in water sources, it is of great significance to accurately trace the source of heavy metal pollution and provide an effective removal technique through rational scientific procedures.

Several techniques have been available to remove heavy metal ions from wastewater prior to being released into the environment. Elimination of heavy metals can be achieved through various methods, including nanofiltration, ion exchange, phytoremediation, chemical precipitation, electrocoagulation, and adsorption [6–12]. Despite the effectiveness of these aforementioned techniques, some parameters contribute to its drawback i.e., sludge generation, maintenance, equipment cost, energy consumption, low efficiency, and time-consuming. By contrast, adsorption is considered the most effective physicochemical technique for heavy metal removal because of its ease of handling, low capital cost, high efficiency, and suitability for both batch and continuous processes [13]. Although the adsorption technique has good heavy metal removal efficiencies, however, its effectiveness depends on the adsorbent type and the ionic concentration of the metalloids. Hence, the sorption reaction is generally considered to be very slow [14]. Some of the adsorbents commonly used are activated carbon (AC), biochar (BC), clay minerals, chitosan, lignin, nanomaterials, and geopolymers [15].

Among various adsorbents, geopolymer has gained a great interest among researchers due to its excellent immobilization effect. Geopolymer is an inorganic polymer with a three-dimensional polymeric structure and pores formed by the condensation of aluminosilicate mineral powder being added into an alkali solution at temperatures below 100 °C. Similarly, the nano-geopolymer structure provides excellent adsorbent properties, which can aid in heavy metal removal from wastewater. Geopolymer has similar properties to zeolite and has a high capacity for cation exchange and a strong affinity for cationic heavy metals with the presence of Al in the geopolymer matrix [16, 17]. In addition, geopolymer can be synthesized by using geological origins such as kaolin, metakaolin, and dolomite and industrial waste such as slag, fly ash (FA), and sludge as an aluminosilicate precursor. Also, nanotechnology is known for removing contaminants through adsorption [18]. However other studies suggested that nanotechnology removes HMs through adsorption, coagulation, and precipitation process [19]. Although, the removal of HMs using nanotechnology could also be achieved through ion exchange or complexation. However, some studies suggested that the effective removal of HMs and metalloids could depend on the proper selection of adsorbents [20, 21].

Ibrahim et al. [22] suggested that nanotechnology offers unique adsorption properties such as different structural selectivity, optimal sorption capacity, and cation exchangeability for various metal cations, which can be used to optimize the process design of wastewater treatment due to its large specific surfaces, sorption capacity, and large surface interactions that mobilize fast adsorption rates.

Mathur et al. [23] assessed the effective removal of Cd, Ni, and Pb from contaminated water by utilizing three silica-based nanomaterials, i.e., non-functionalized silica nano hollow sphere (SNHS), amino-functionalized silica gel (NH2-SG), and amino-functionalized silica nano hollow sphere (NH2-SNHS). According to their results, their investigation concluded that the adsorption capacities of the 3-nanomaterials were in the order of NH2-SNHS > NH2-SG > SNHS with associated metal removal through adsorption of Pb (II) > Cd (II) > Ni (II). The maximum adsorption capacities for Pb (II), Cd (II), and Ni (II) were achieved using NH2-SNHS was 96.79, 40.73, and 31.29 mg·g⁻¹ respectively. Other than the application of nanotechnology in the removal of HMs, some studies have supported the use of recycled waste materials due to their value-added adsorbent efficiency. This requires careful execution and selection to mitigate overdosing of the contaminated water. Kumara and Kawamoto [24] investigated the removal of HMs through the synergy effects of clay and slag. They reported that the combination of crushed waste clay bricks (CCB) and municipal solid waste slag (MSWS) recorded appreciable heavy metal adsorption from highly concentrated wastewater in their study. Among these, their study suggested that the adsorption of HMs using CCB and MSWS was mainly controlled by deprotonation at a neutral pH value. Whereas, at a pH value between 7 and 9, metalloids like Cd²⁺ and >7 for Pb²⁺, were 60% removed from the wastewater as the traces of these metalloids dominated the surface of the adsorbents forming precipitate-like crystals.

Nguyen et al. [25] activated class “C” fly ash using 2-mercaptobenzothiazole (MBT) and sodium dodecyl sulfate (SDS) as the surfactants after treatment with 1M NaOH solution. Their study concluded that the number of adsorbed ions of the activated fly ash was 68% higher on average than that of the unmodified fly ash. The activated fly ash showed the capability of adsorbing toxic metals because its oxides and hydroxides are capable of providing adsorption sites for anions.

According to available literature, it is established that the adsorption technique is widely accepted, but the process that guides the complete rate of the sorption process is slow. As such, the adsorption kinetics forms an integral part sorption reaction because it provides information on the rate at which metalloids are absorbed. This is the gap this study attempted to bridge by investigating the efficiency of heavy metal adsorption and also studying the important parameters such as concentration of nanomaterial, solid-to-liquid ratio, equilibrium period, and the temperature required for the complete pozzolanic process. Therefore, to understand the adsorption capacity of the nano-slag clay liner (adsorbent), the following factors were investigated, the effect of pH on heavy metal adsorption and percentages of absorbed HM ions using pseudo-second-order model [26]. Furthermore, Ahmadi et al. [27] suggested that the pseudo-second order of kinetic reaction rate depends on the mass of the metalloids on the sorbent surface as well as the quantity of adsorbed metal ions at equilibrium. This model is widely employed for the study of chemisorption kinetics for liquid solution systems [28]. Therefore, chemisorption was employed in this study, since it involves the interaction between nanomaterial (adsorbent) and contaminated water (adsorbate) through chemical reactions, which create covalently. This study mainly targeted the removal of As, Cd, and Pb, however, the removal of other HMs and metalloid were also investigated. The choice for selecting adsorbent was mobilized by its capacity to increase the pH level of the entire chemisorption through adsorption, precipitation, and coagulation of metallic ions.

2. Materials and Methods

2.1. Natural soil

The soil used for this study is natural Bentonite clay collected from Mpumalanga in South Africa at a depth of 1.2 m without any form of contamination. The collected soil was oven-dried for 24 hours at a temperature of 24°C to eliminate hygroscopic moisture that might have been trapped within the soil voids. ASTM D1140 [29] test protocol was followed to perform a sieve analysis test. Subsequently, different particles retained in sieve sizes of 9.5 mm and 4.75 mm, were used to determine the percentages of gravel and sand. The percentage of the fine was also determined on the soil particle size of 75µm following hydrometer analysis. The percentages of clays and silts were further evaluated; hence the soil's particle size distribution curve is presented in Figure 1. The studied soil has a symbol of CL, this implies that it is clay soil with low plasticity, according to the Unified Soil Classification System (USCS).

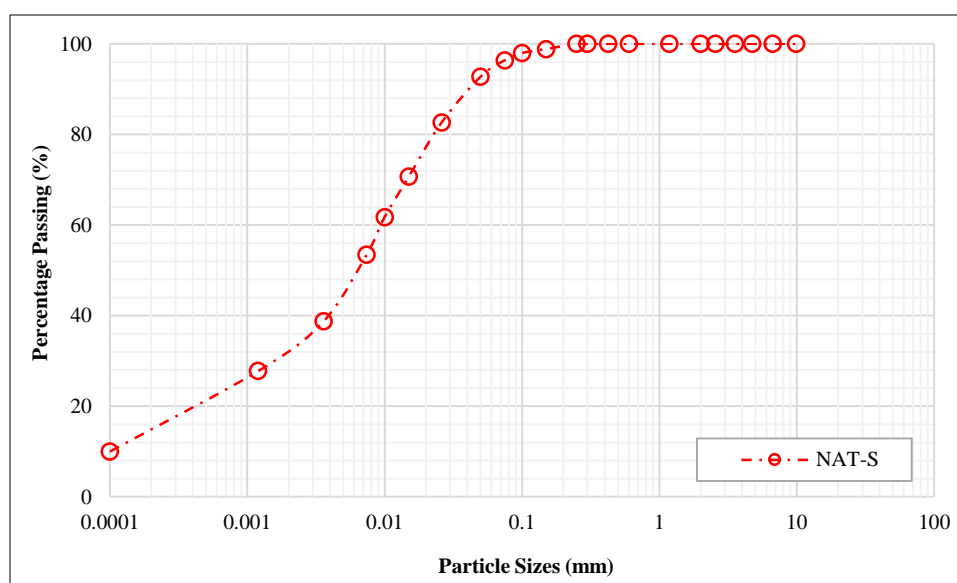


Figure 1. Soil gradation curve

The X-ray fluorescence (XRF) test was also performed to evaluate the chemical compositions of the NAT-S. The test results revealed the selected NAT-S possessed SiO₂, Al₂O₃, + Fe₂O₃, and CaO as the dominant chemical compounds. Following the cation exchange capacity (CEC) which was also performed following Indian Standard, IS 2720-24 [30]. An ammonium chloride solution of 485±3 ppm content equivalent to NH₄⁺ concentration, to determine the total negative charge and CEC of the NAT-S. The result showed that the NAT-S contained fine particles greater than >65%. This indicates that the NAT-S has a positive surface charge for cation exchange with a corresponding value of 48.37 meq/100 g. The value implies that the soil constitutes OH⁻ ion concentration on the surface charge and the sufficient charged hydroxyls (H⁺ ion) capable of losing at the surface. Based on the obtained CEC result, the soil is suspected to possess a little to medium adsorption capacity for heavy metals.

2.2. Nano-Blast Furnace Slag (NBFS)

The steel slag used herein is a basic-oxygen-furnace (BOF) slag acquired from a single batch and supplied by Fry' Metals in South Africa. It constitutes of CaO, MgO, MnO, and FeO to a total oxide of 70% according to the XRF test result. This confirms that the slag used was produced through the process of basic oxygen-furnace (BOF) slag. The slag possesses a particle size of less than 15.3 mm with an average initial moisture content of 7.5%. The slag could not be obtained on a nanoscale level; therefore, the obtained slag was synthesized to a nanoscale using the top-to-bottom method. The nanoscale of the slag starts by drying it in an open-air environment for 7 days followed by mechanical jaw crushing. The slag was first crushed into a granular size of <4mm followed by continuous grinding in a mechanical ball-milling. The milling process lasted for 6 h with 0.5 h intervals at a rotation of 500rpm. Toluene and anionic surface-active chemical agents were added at each interval to cool the inner chamber of the mill and eliminate any form of agglomerations that might be formed by the slag nanoparticles. These conditions were repeated for each run until the surface area of the nano-slag particles increased from 0.02 m²/gm to 23.40 m²/gm according to the high-resolution transmission electron microscopy (HRTEM) analysis, with the particle sizes of nanosized slag evaluated within the range of >10 nm. The preliminary test results presented in Table 1 was essentially used to quantify the quantity of clay minerals in the soil which was used to develop the nano-slag clay liner (NSCL). Unfortunately, the soil possesses little capacity to adsorb the heavy metals and metalloids according to its CEC, pH value, and nano-size.

Table 1. Chemical composition of NAT-S and NBFS

Materials	XRF							
	SiO ₂	Al ₂ O ₃	Fe ₂ O ₃	CaO	K ₂ O	MgO	Others	CEC (meq/100 g)
NAT-S	52.59	17.41	12.38	6.62	4.95	4.40	1.65	75
NBFS	17.41	5.21	28.24	38.68	1.4	6.3	2.77	298
Mineralogical compositions XRD								
	Smectite	Phyllosilicate	K-feldspar	Plagioclase	Illite	Calcite		
NAT-S	71.74	13.41	9.91	1.85	1.89	1.22	>>	
	Merwinite	Olivine	Wüstite	Brownmillerite	Larnite	Vaterite		
NBFS	51.13	43.24	33.23	23.11	18.21	11.21	>>	

2.3. Contaminated Water

Samples of the contaminated water were collected from a single source near an active mine in Mpumalanga, South Africa. The pictorial view of the contaminated water site is presented in Figure 2. The water body was suspected to be contaminated with acid mine drainage due to nearby mining activities coupled with adverse impacts on the vegetation and plants within the surrounding environment. Crystal salt formation was visible on the contaminated water surface protrusions, as the contaminated water was collected from different locations to have a wide representation of the contaminated water samples. The salt-like crystals formation are heavy metals that were noted as dissolved ions in the contaminated water.



Figure 2. Site setup of the investigated acid mine drainage

The contaminated water source was monitored on-site for 24 months using an acid concentration meter to determine its concentrations. The variation in concentration over time for the contaminated water is shown in Figure 3. The lowest pH value of 2.5, was recorded as the lowest [H⁺] concentration of the sampled contaminated water over 2 years, therefore qualifying the contaminated water sample as acidic water.

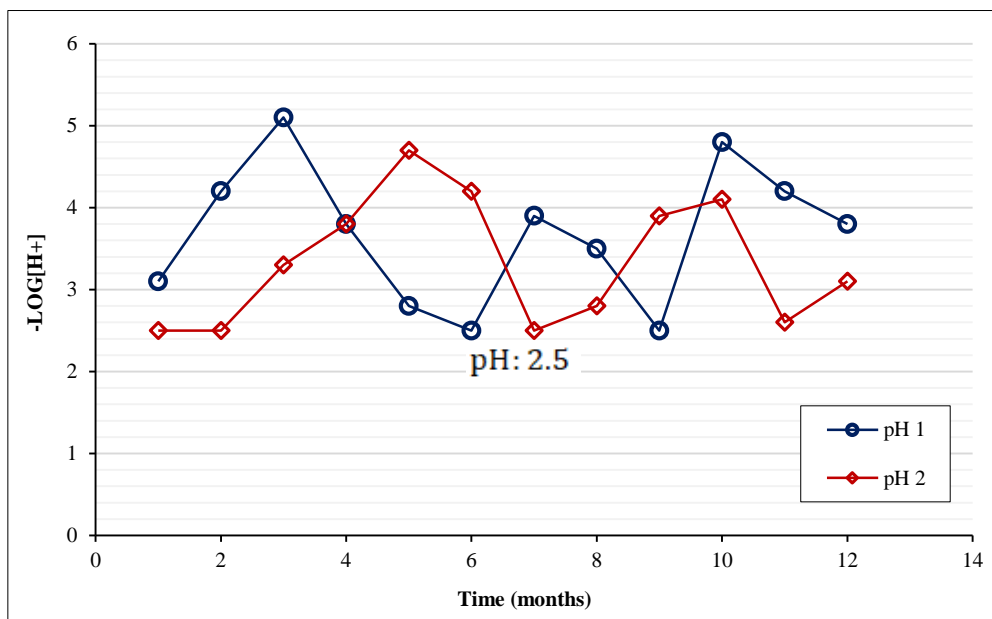


Figure 3. Site setup of the investigated acid mine drainage

A series of chemical composition and concentration evaluations were performed on the collected contaminated water samples using ICP-MS and the results are summarized in Table 2. The test result confirmed that the contaminated water rendered a high electrical conductivity and contained elevated levels of sulphate and dissolved heavy metals. Also, the concentration of HMs and metalloids contained in the contaminated water were beyond the concentration ions limit specified by WHO [2] and DWARF [31] for livestock, watering, and irrigation/construction as demonstrated in Table 2. The HMs and metalloids like As, Cr, Hg, Fe, Pb, Cu, Cd, and Ni were contained in the contaminated water with their concentrations above the permitted limits for agricultural and irrigation/construction purposes. Thus, studies have suggested that the major water contaminants are Arsenic (As), Cadmium (Cd), Chromium (Cr), Lead (Pb), Mercury (Hg), Thallium (Tl), and Nickel (Ni) [31].

Table 2. Chemical composition of raw AMD, water quality standards (DWARF, 1996)

Element	pH	Hg	Fe	As	Zn	Pb	Cu	Cd	Ni	Cr	SO ₄
Concentration (Mgdm ⁻³)	2.5	14	32	6.0	5.41	15.3	22	39.3	14.4	<0.5	1280
Livestock watering (Mgdm ⁻³)	6.5-8.5	1.0	10	1.0	20	0.5	5.0	10	1.0	1.0	1000
Irrigation (Mgdm ⁻³)	6.5-8.5	<<	5.0	0.001	1.0	0.2	0.2	10	0.20	0.05	<<

3. Methods

The pH test was performed to measure the effects of proton in aqueous solutions and to evaluate the changes in pH values (alkalinity) of the contaminated water when interacting with the NSCL. The ASTM D6276 [32] protocol was followed to achieve this task, as four calibrated conical glass jars containing the solution of NBFS and soil to the combined ratios of 90:10; 80:20, 70:30, 60:40, and 50:50. The maximum soil particles size selected for this test is 425µm. The calibrated conical glass jars were set up to contain 50g of NSCL and 200 ml of the contaminated water. The solutions were agitated for 25 mins and allowed to settle before insertion of the pH meter to measure the pH values from each jar. The test results revealed that the pH values of the investigated contaminated water increased as the percentages of NBFS content increased in the clay liner mixture. A significant increase in pH values was noted at a 50:50 soil: NBFS ratio, beyond which the pH value remains stable as presented in Figure 4. The pH value indicated that the nano-slag clay liner developed with 50% of clay and 50% NBFS recorded a pH value of 13.10. This implies that under this combined ratio higher cations exchange capacity by anionic charge was achieved compared to the rest of the clay liner.

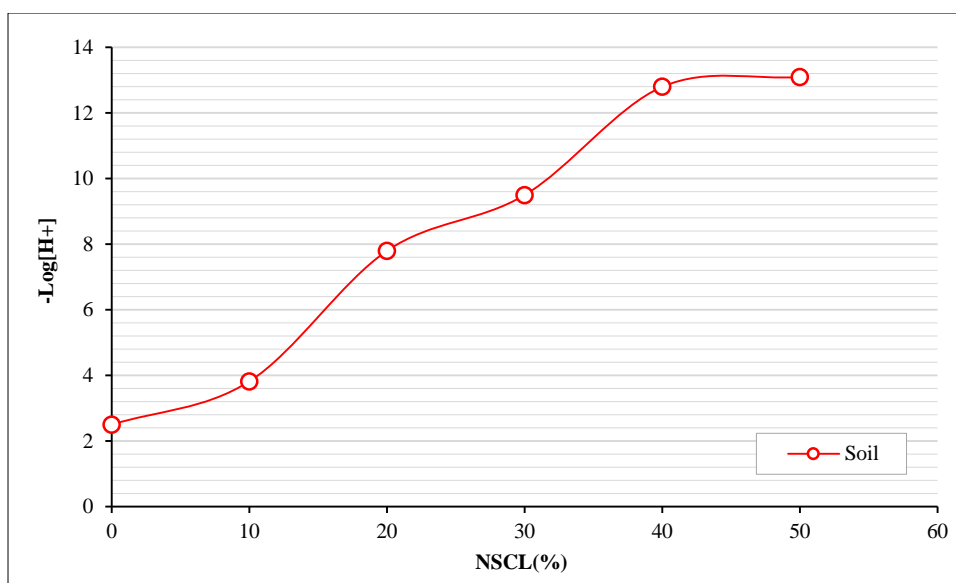


Figure 4. pH interaction of nanosized- slag clay liner with the contaminated water

3.1. Experimental Setup and Testing Procedure

The leachate test was performed in this study to adsorb the targeted heavy metals i.e. As, Cd, and Pb. The methodological process was achieved by first blending nano-slag, and Bentonite soil in a varying ratio of 90:10; 80:20, 70:30, 60:40, and 50:50 to the combined mass of soil and nano-blast furnace slag (NBFS) followed by a slight addition of water. The blends were thoroughly mixed for 15 minutes until a homogenous mixture was achieved forming a nano-slag clay liner. The material was placed and compacted into the attenuation at a temperature of 50°C. The temperature was selected to improve the rate of sorption as well as to enable the complete development of the tertiary compound through a polymerization reaction. Figure 5 illustrate the methodological flowchart of the leachate test.

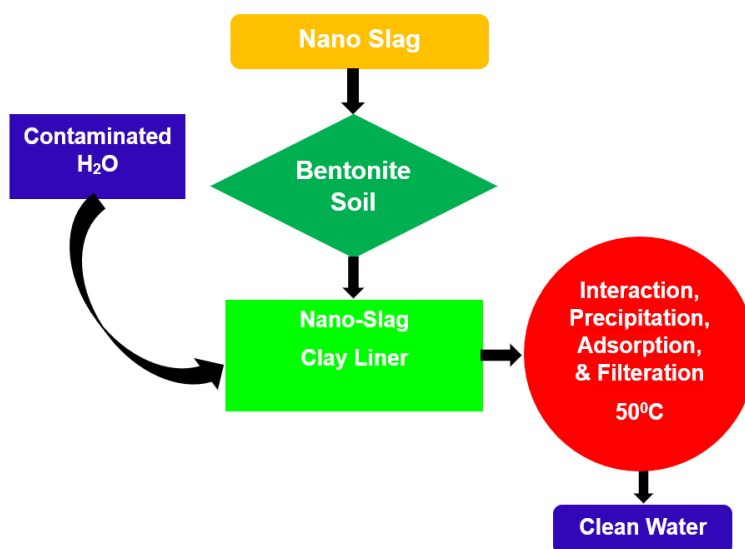
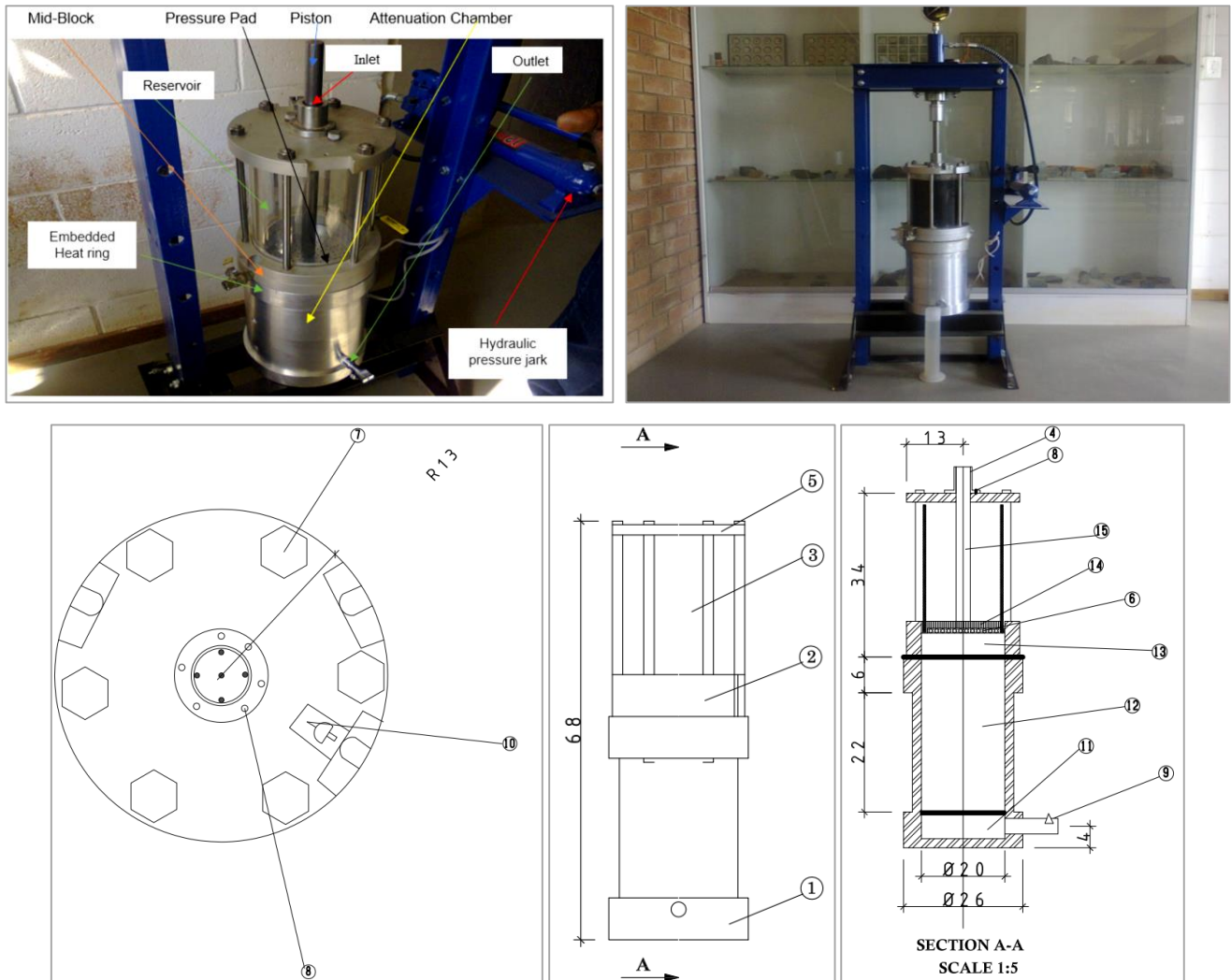


Figure 5. Methodological process of the leachate test

The adsorption HMs from the contaminated water was achieved using the Leachate Modular Tower. The nano-slag clay liner was compacted into the attenuation chamber of the LMT. Firstly, washed gravel aggregates between 2 mm to 2.5 mm sizes were placed at the bottom section of the attenuation chamber and a non-woven filtration geotextile material was placed on top of the gravel. The filtration material was selected to allow an easy flow of the contaminated water while preventing the NSCL particles from passing through. The testing was structured in a framework such that the NSCL was uniformly compacted into the attenuation chamber to serve as a liner after the gravel aggregates, and non-woven filtration geotextile material were placed into attenuation chamber. The perforated pressure pad was placed on the top of the attenuation chamber to aid the distribution of the contaminated water across the circumference of the compacted nano-slag clay liner in the attenuation chamber. The contaminated water was placed in the reservoir and the LMT was coupled to avoid spillage. The equipment was powered and the internal temperature of 50°C was maintained

using the embedded heating ring around the lower block of the reservoir. This temperature was chosen based on the study published by Dubey et al. [33] which concluded that a constant temperature of 50°C plays a key role in the adsorption process of HMs and metalloids. Also, the equilibrium adsorption capacity of nanomaterials is expected to alter at elevated temperatures to mobilize the redox reaction rate. The experimental setup and schematic diagrams of the built LMT are shown in Figure 6.



Name	Part	QTY
Pressure Piston	15	1
Porous Pressure Plate	14	1
Sample Holder	13	1
Attenuation Chamber	12	1
Porous Stone Chamber	11	1
Clip	10	1
Effluent	9	1
Standard Nut	8	6
Standard Nut	7	6
Geosynthetic Material	6	1
Lid	5	1
Influent	4	1
Leechate Chamber	3	1
Mid Block	2	1
Lower Block	1	1

Figure 6. Schematic diagram of Modular Leachate Tower

After the setup of the LMT equipment, the contaminated water was retained in the attenuation chamber at different equilibrium adsorption periods of 2, 5, 7, and 10 days to investigate the effects of the attenuation period on the sorption capacities of the NSCL. After the equilibrium period was attained, the outlet was opened, and the contaminated water that leached through the liner was collected using a graduated cylinder. As another inductive coupled plasma mass spectrometry (ICP-MS) test was performed to measure the concentration of HMs and metalloid ions in the collected leached water. The number of heavy metal ions adsorbed per gram of adsorbent, Q ($\text{mg}\cdot\text{g}^{-1}$), was calculated using Equation 1.

$$Q = \frac{(C_0 - C_e)V}{W} \quad (1)$$

where Q is the amount of adsorbed metal ion at equilibrium conditions (metal ion (mg)/adsorbent (g)), V is the solution volume (L), and W is the sorbent mass (g). C_0 and C_e are the initial and equilibrium concentrations of metal ions in solution ($\text{mg}\cdot\text{L}^{-1}$), which are determined by the ICP-MS test. To calculate the percentage removal of metal ions, pseudo-first-order kinetic was applied as expressed in Equation 2.

$$H = \frac{(C_0 - C_e)}{C_0} \times 100 \quad (2)$$

where H is the percent removal of metal ions (%), all experiments were performed in triplicate and the average value was recorded as the final test result.

The scanning electron microscopy (SEM) test was conducted on the NSCL to evaluate the surface morphology of the untreated natural soil liner and NSCL. The SEM test enables the high-resolution imaging of nanoparticles with sizes below 10 nm. High-resolution image was achieved from the upper-most surface of the NSCL by advanced detectors. The SEM machine used herein is the VEGA3 TESCAN-6480 scanning electron microscope operated at 20kV. The test was successfully conducted due to the capacity of SEM equipment to measure lateral dimensions on the nano-scale.

4. Results and Discussion

4.1. Adsorption Capacity of The Natural Soil

The capacity of the natural soil to adsorb HMs was evaluated at different attenuation periods using Equation 1. The reduction of HM ions concentration after the interaction period between the natural soil and contaminated water at different attenuation periods is presented in Table 3. The results showed that the natural soil through ion exchange and adsorption mechanisms slightly removed the cations and anions of few metalloids at 10 days of equilibrium periods. Whereas no adsorption of HMs was achieved at 2, 5, and 7 days respectively. In furtherance, the degree of HMs concentration after 2 and 5 days of interaction periods are higher compared to the standard stipulated by DWARF [31], and WHO [2]. Whereas, at 7 and 10 days of interaction periods, the concentrations of the targeted metalloids ions i.e., as Cr(VI), As(III), and Pb(II) remained unchanged whereas slightly decrease Cd, Cu, and Hg ions concentration were recorded. The low adsorption of HMs by the natural soil is associated with the inability to high exchangeable cations and anions on the soil surface. Furthermore, the low surface area and pore volume were also noted to be part of the contributing factor for low adsorption capacity of clay.

The result obtained in this study agrees with the report published by Chen et al. [34], and Zacaroni et al. [35], which suggested that microstructure, and high cation exchange capacity (CEC) improves the adsorption capacity of a soil. The hierarchy of the natural soil is in the order of sorption $\text{Cd} > \text{As} > \text{Pb}$. However, no adsorption activities were noted for Cr, Zn, Ni, As, and Fe ions after 10 days of the interaction process. It was also noted that the concentration of Cu and Hg were reduced by 33% and 38% respectively with no change in concentration ion for SO_4 . This could be attributed to the percentage of free aluminium phyllosilicate minerals available in the soil as well as the diffused double layer within the outer surface structure and the elevated temperature. In addition, study by Campillo et al. [36] supported that the uptake of heavy metals by clay minerals involves a series of complex adsorption mechanisms, such as direct bonding between metal cations with the surface of clay minerals, surface complexation, and ion exchange [37]. The soil use herein was noted to achieved low adsorption of HMs, this implies that the soil requires pre-treatment and modification to enhances the surface area, pore volume, and CEC on the surface for effective adsorption of HMs.

Table 3. Quantities of absorbed heavy metals by non-treated clay liner

HMs	Initial Conc. (Mgdm ⁻³)	Effluent @ 2 days (Mgdm ⁻³)	Effluent @ 5 days (Mgdm ⁻³)	Effluent @ 7 days (Mgdm ⁻³)	Effluent @ 10 days (Mgdm ⁻³)	DWARF, 1996 (Mgdm ⁻³)		WHO(Mgdm ⁻³)
						Livestock	Irriga.	Drinking water
Hg	14.0	11.52	9.35	5.23	0.95	1.0	>>	0.001
Fe	32.0	32.0	32.0	32.0	20.10	10.0	5.00	>>
As	9.00	9.00	9.00	9.00	9.00	1.00	0.01	0.001
Zn	5.41	5.41	5.41	5.41	5.41	20.0	1.00	>>
Pb	15.3	10.42	8.31	4.24	0.120	0.50	0.20	0.010
Cu	22.0	17.64	15.2	10.12	2.140	5.00	0.20	2.000
Cd	39.3	22.69	17.14	11.40	3.41	10.0	10.0	0.003
Ni	14.4	14.4	14.4	14.4	14.40	1.00	0.20	>>
Cr	0.50	0.50	0.50	0.50	0.50	1.00	0.05	0.050
SO ₄	1280	1280	1280	1280	1280	1000	>>	>>

*WHO: World Health Organization

4.2. Adsorption of HMs by Nano-Slag Clay Liner (NSCL)

Nanomaterials has been extensively studied for the removal of heavy metals and metalloids due to their large specific surface areas with enhanced active sites for contaminant adsorption [38]. The results indicated that the rate sorption of the nano-slag clay liner improved significantly causing decrease in concentrations and quantities of the HM ions at several contact times. Table 4 portrayed a high adsorption order of 98%As>, 99%Cd>, and 99.9%Pb> at 10 days equilibrium time with adsorbent ratio of 50: 50 clay and nano-slag. The results further revealed that the metalloids like Cu>, Zn>, Hg>, Ni> Fe>, and Cr> were greatly adsorbed at the same equilibrium period and nano-slag clay dosage. At interaction period of 2 days, the concentration of HMs ions was slightly decreased. The adsorption trend portrayed significant increase of adsorbate (heavy metals) as the interaction time continue to increase, the concentration of HMs ions decreased. A significant decrease in ionic concentration was noted at 7 and 10 days of interaction time. For example, Hg had an initial ion concentration of 14 Mgdm⁻³, upon 2 days of interaction period, the ion concentration decreased from 14 Mgdm⁻³ to 6.14 Mgdm⁻³. Thus, further decrease in ion concentration was noted at 5, 7, and 10 days of interaction time resulting to decrease values of further from 2.15 Mgdm⁻³, 0.001 Mgdm⁻³, and 0.001 Mgdm⁻³ respectively

Table 4. Concentration of absorbed HM ions by 50: 50 NSCL

HMs	Initial Conc. (Mgdm ⁻³)	Effluent @ 2 days (Mgdm ⁻³)	Effluent @ 5 days (Mgdm ⁻³)	Effluent @ 7 days (Mgdm ⁻³)	Effluent @ 10 days (Mgdm ⁻³)	DWARF, 1996 (Mgdm ⁻³)		WHO (Mgdm ⁻³)
						Livestock	Irriga.	Drinking water
Hg	14.0	6.14	2.15	0.001	0.001	1.0.	>>	0.001
Fe	32.0	20.2	18.0	4.31	2.14	10.0	5.00	>>
As	9.00	5.11	2.14	0.001	0.001	1.00	0.01	0.001
Zn	5.41	2.21	1.08	0.88	0.38	20.0	1.00	>>
Pb	15.3	8.14	3.42	0.18	0.11	0.50	0.20	0.010
Cu	22.0	13.2	7.42	1.24	1.00	5.00	0.20	2.000
Cd	39.3	20.2	11.22	3.10	0.41	10.0	10.0	0.003
Ni	14.4	9.21	3.12	0.20	0.20	1.00	0.20	>>
Cr	0.50	0.35	0.15	0.05	0.03	1.00	0.05	0.05
SO ₄	1280	1120	950	758	758	1000	>>	>>

*WHO: World Health Organization

In Tables 5 to 8 similar decreasing trends were observed upon the evaluation of HM ions concentrations various clay and nano-slag ratios of 60:40, 70:30, 80:20, and 90:10 as the adsorbent and NBFS liners at various interaction periods. The result shows great proportionality between the adsorption of HM ions and the nanomaterial. The decrease in HM ion concentration occurred as the nano-slag content increases and decreases when clay content increases. The adsorption of the HMs and metalloids were significant at 7 days of interaction times beyond which the HMs ions concentrations remained unchanged. Also, it was noted that the variation and effects of HM ions quantities decrease with an increase in pH value and initial metal ion concentration. For instance, the removal of Cd is higher compared to Hg with a lesser initial ion concentration, hence the adsorption capacity at 7 days for Cd is 36.2Mgdm⁻³ whereas in Hg an adsorption capacity of 13.99 Mgdm⁻³ was recorded. These results indicated that the actual amount of HM ions absorbed per unit

mass of the absorbent increased with metal ion concentration. The adsorption trend observed in this study is associated to large surface area, high sorption capacities, temperature range and the adsorption capacity of nano-slag. The surface area of the nano-slag mobilized the wide range sorption capacity for the system, suggesting its potential for treating contaminated water. The results obtained in this study are related to other studies [38-44] which stated that nanomaterial adsorbents are active for heavy metal removal due to their large specific surface areas with enhanced active sites for contaminant adsorption and effective adsorbent in continuous adsorption mode. These concluded that nanomaterials have many unique morphological and structural properties that mobilises effective adsorbents of heavy metals at the outer surface.

Table 5. Concentration of absorbed HM ions by 60: 40 NSCL

HMs	Initial Conc. (Mgdm ⁻³)	Effluent @ 2 days (Mgdm ⁻³)	Effluent @ 5 days (Mgdm ⁻³)	Effluent @ 7 days (Mgdm ⁻³)	Effluent @ 10 days (Mgdm ⁻³)	DWARF, 1996 (Mgdm ⁻³)		WHO (Mgdm ⁻³)
						Livestock	Irriga.	Drinking water
Hg	14.0	8.31	4.21	0.01	0.001	1.0.	>>	0.001
Fe	32.0	24.0	21.0	4.71	3.21	10.0	5.00	>>
As	9.00	5.12	4.14	0.81	0.001	1.00	0.01	0.001
Zn	5.41	2.10	1.23	0.94	0.67	20.0	1.00	>>
Pb	15.3	9.10	9.41	0.75	0.18	0.50	0.20	0.010
Cu	22.0	15.0	14.0	10.21	5.00	5.00	0.20	2.000
Cd	39.3	22.0	18.22	13.0	8.10	10.0	10.0	0.003
Ni	14.4	10.18	6.31	2.18	0.90	1.00	0.20	>>
Cr	0.50	0.40	0.25	0.05	0.05	1.00	0.05	0.05
SO ₄	1280	1260	1200	1150	1000	1000	>>	>>

*WHO: world health organization

Table 6. Concentration of absorbed HM ions by 70: 30 NSCL

HMs	Initial Conc. (Mgdm ⁻³)	Effluent @ 2 days (Mgdm ⁻³)	Effluent @ 5 days (Mgdm ⁻³)	Effluent @ 7 days (Mgdm ⁻³)	Effluent @ 10 days (Mgdm ⁻³)	DWARF, 1996 (Mgdm ⁻³)		WHO (Mgdm ⁻³)
						Livestock	Irriga.	Drinking water
Hg	14.0	9.11	6.15	2.10	0.88	1.0.	>>	0.001
Fe	32.0	26.2	22.0	5.00	4.00	10.0	5.00	>>
As	9.00	7.11	3.00	0.83	0.03	1.00	0.01	0.001
Zn	5.41	3.21	2.18	1.21	1.02	20.0	1.00	>>
Pb	15.3	10.0	8.12	1.25	0.53	0.50	0.20	0.010
Cu	22.0	17.0	15.1	12.0	7.00	5.00	0.20	2.000
Cd	39.3	24.0	22.0	15.0	9.0	10.0	10.0	0.003
Ni	14.4	13.0	7.00	3.21	1.0	1.00	0.20	>>
Cr	0.50	0.43	0.35	0.05	0.05	1.00	0.05	0.05
SO ₄	1280	1263	1200	1152	1000	1000	>>	>>

*WHO: world health organization

Table 7. Concentration of absorbed HM ions by 80: 20 NSCL

HMs	Initial Conc. (Mgdm ⁻³)	Effluent @ 2 days (Mgdm ⁻³)	Effluent @ 5 days (Mgdm ⁻³)	Effluent @ 7 days (Mgdm ⁻³)	Effluent @ 10 days (Mgdm ⁻³)	DWARF, 1996 (Mgdm ⁻³)		WHO (Mgdm ⁻³)
						Livestock	Irriga.	Drinking water
Hg	14.0	9.30	7.00	2.30	0.90	1.00	>>	0.001
Fe	32.0	27.0	22.11	5.20	5.00	10.0	5.00	>>
As	9.00	7.41	3.50	1.0	0.04	1.00	0.01	0.001
Zn	5.41	3.22	2.20	1.24	1.12	20.0	1.00	>>
Pb	15.3	11.2	8.31	1.35	0.58	0.50	0.20	0.010
Cu	22.0	17.2	15.3	12.3	7.20	5.00	0.20	2.000
Cd	39.3	24.2	22.3	15.2	9.2	10.0	10.0	0.003
Ni	14.4	13.2	7.20	3.40	1.00	1.00	0.20	>>
Cr	0.50	0.43	0.35	0.05	0.05	1.00	0.05	0.05
SO ₄	1280	1265	1210	1155	1000	1000	>>	>>

*WHO: world health organization

Table 8. Concentration of absorbed HM ions by 90: 10 NSCL

HMs	Initial Conc. (Mgdm ⁻³)	Effluent @ 2 days (Mgdm ⁻³)	Effluent @ 5 days (Mgdm ⁻³)	Effluent @ 7 days (Mgdm ⁻³)	Effluent @ 10 days (Mgdm ⁻³)	DWARE, 1996 (Mgdm ⁻³)		WHO (Mgdm ⁻³)
						Livestock	Irriga.	Drinking water
Hg	14.0	10.1	9.0	4.23	0.90	1.0	>>	0.001
Fe	32.0	27.1	22.2	5.25	5.00	10.0	5.00	>>
As	9.00	7.45	3.55	1.10	0.35	1.00	0.01	0.001
Zn	5.41	3.25	2.25	1.28	1.18	20.0	1.00	>>
Pb	15.3	11.4	8.31	4.24	0.12	0.50	0.20	0.010
Cu	22.0	17.3	15.4	12.4	2.10	5.00	0.20	2.000
Cd	39.3	24.3	17.2	11.4	3.41	10.0	10.0	0.003
Ni	14.4	13.4	7.25	3.41	1.00	1.00	0.20	>>
Cr	0.50	0.45	0.35	0.05	0.50	1.00	0.05	0.050
SO ₄	1280	1270	1220	1160	1000	1000	>>	>>

*WHO: world health organization

4.3. Effect of pH on Heavy Metal Adsorption

The effects of pH HMs adsorption with nano-slag variation are presented in Figures 7 to 11. The test results revealed that the pH has a significant influence on the adsorption process of heavy metals and metalloids, as it acts on the functionality and could impact their sorption rates. The results revealed that increasing the dosages of the nano-blast furnace slag in the mix mobilized an increase in pH values from 2.5 to 5.13, 7.23, 10.41, 11.18, and 13.1 upon the inclusion of 10%, 20%, 30%, 40%, and 50% nano-blast furnace slag. The increase in the nano-blast furnace slag resulted in a significant uptake of HM ions. This implies that nano-slag contents control the pH levels, which in turn influence the sorption process. Therefore, at a low pH level, the mobility of metal ions in the wastewater is higher, whereas, at a higher pH, the lower mobility of Cd, As, Pb, and other metalloids is established by Zhang et al. [45]. The surface area of the nano-slag used herein played a critical role in determining the potential for a given quantity of adsorbed HM ions. For instance, a 50:50 ratio of soil and nano-slag increased the pH level from 2.5 to 13.1 and caused a decrease in the HM ion concentration of Cd from 39.3 mg dm⁻³ to 20.2 mg dm⁻³ for 2 days interaction period. According to the presented curves, the red color indicates a high-level HMs concentration at low pH values. Therefore, increasing the contents of the nano-slag dosages, caused a significant decrease in HMs ion concentration as the pH level increased. The increase in nano-slag dosage mobilized color changes and a reduction in the concentration of HMs, as shown by the curve legends. The color was noted to change from red to orange and further change from orange to yellow, green, and finally purple. These color changes imply significant uptake of HM ions until the optimum level of HM ions is adsorbed at elevated pH values.

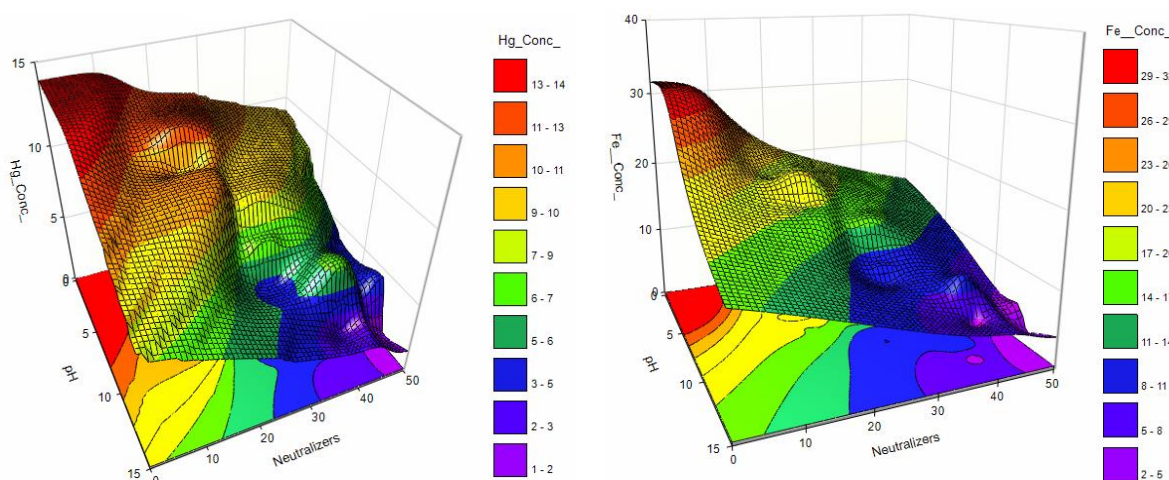


Figure 7. Variation of pH and adsorption of Hg and Fe from AMD with different absorbent doses

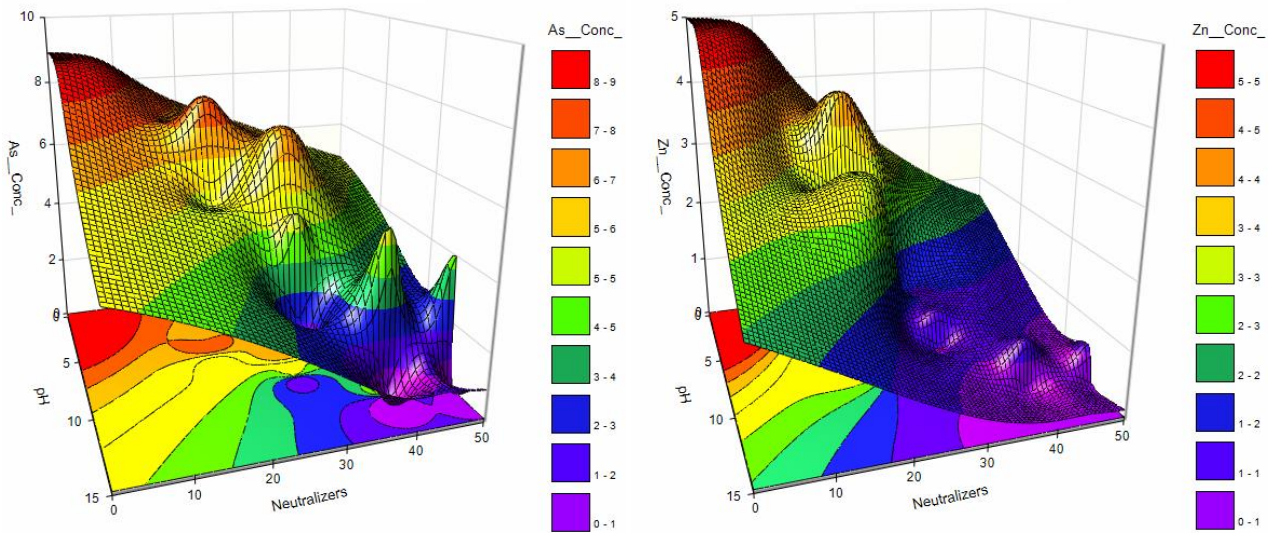


Figure 8. Variation of pH and adsorption of As and Zn from AMD with different absorbent doses

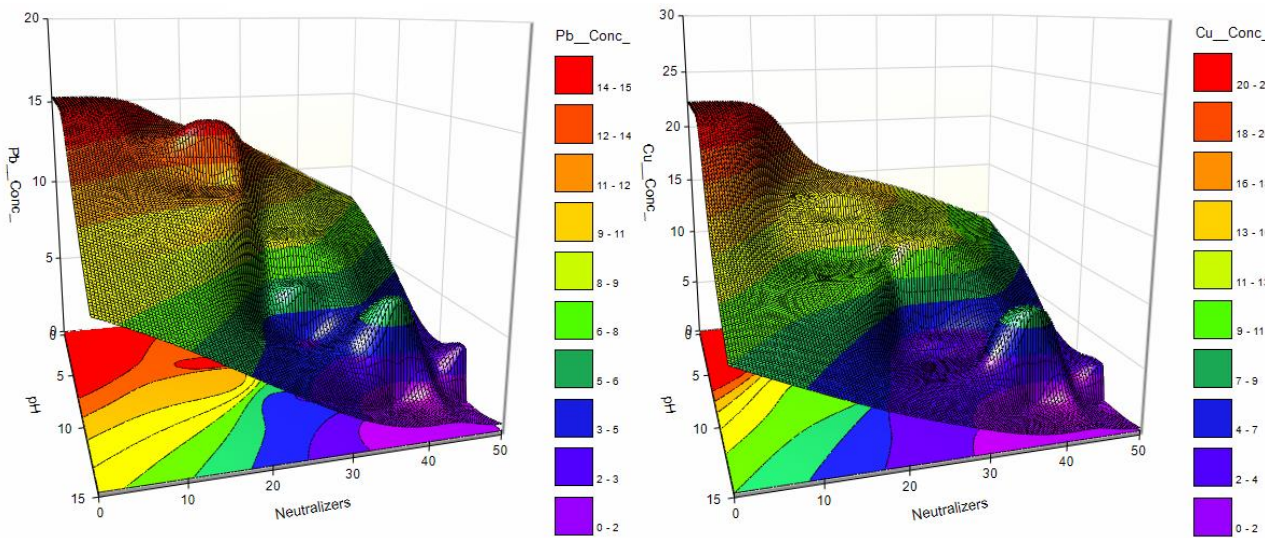


Figure 9. Variation of pH and adsorption of Pb and Cu from AMD with different absorbent doses

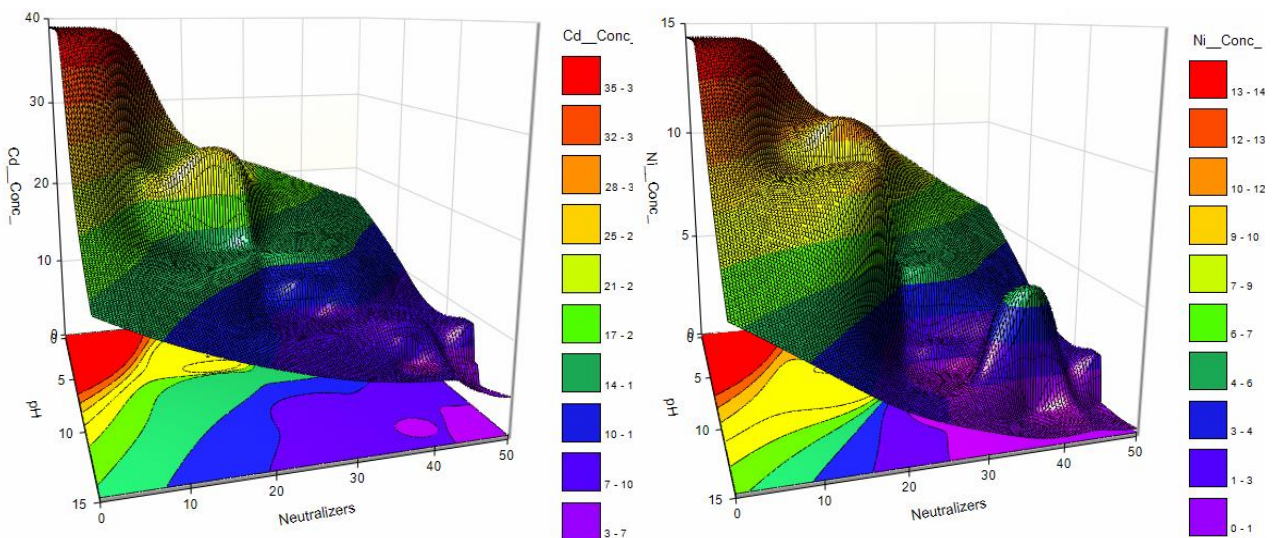


Figure 10. Variation of pH and adsorption of Cd and Ni from AMD with different absorbent doses

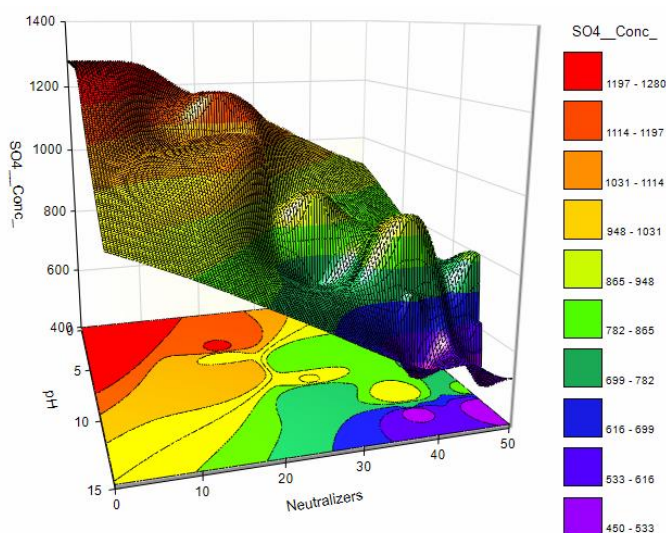


Figure 11. Variation of pH and adsorption of SO4 with different absorbent doses

Generally, the high adsorption of HM ions was possible due to the increase in pH which was triggered by the pozzolanic reaction between the soil and nano-slag. The pozzolanic reaction formed tertiary compounds such as dicalcium silicate (C₂S), tricalcium silicate (C₃S), and free calcium oxide (f-CaO) in steel slag. These tertiary compounds possess excellent alkalinity in the CSH. The alkalinity in the tertiary compounds triggers the increase in the pH value of the framework from 2.5 to 13.1. This also mobilized the precipitation of HM ions at elevated temperatures during the interaction time, forming insoluble hydroxide within the pores of the clay layer. The effects of pH values on the adsorption of HMs and metalloids observed in this study trend agrees with the report published elsewhere [46-51], which confirms that increased pH level, triggers an increase in the sorption rate of HM ions through which precipitation occur on the surface of the adsorbent. The results obtained here are comparable to the study published by Yadav et al. [52] which stated that the application of nanomaterial for wastewater treatment increases the sorption rate of heavy metals with a significant influence on the temperature. The small particle size effect was noted to improve the reaction between the nano-slag and clay minerals which resulted in favorable uptake of the targeted metalloids.

4.4. Percentages of Absorbed HM Ions

Figures 12 to 15 present the sorption capacity of the NSCL using Equation. 2. The ratio of 50% clay and 50% nano-slag at various interaction times was selected to evaluate the adsorption efficiency of NSCL. It was noted that high sorption capacity has great proportionality with interaction time. Also, the adsorption efficiency was noted to increase with interaction. Furthermore, the absorbed percentages of HM ions were significantly influenced by initial concentration rate, CEC, surface area, elevated pH, and surrounding temperature in the LMT. For instance, at an equilibrium period of 2 days, Hg, Fe, As, Zn, Pb, Cu, Cd, Ni, and Cr, the adsorption efficiency of 49%, 31%, 43.3%, 59.2%, 47%, 40%, 49%, 36.4%, and 30% respectively. However, significant adsorption was observed at interaction time between 7 days to 10 days with recording adsorption efficiency of 99.9%, 93.3%, 99.9%, 93%, 99.8%, 95.4%, 99%, 99%, 97%, and 99% respectively.

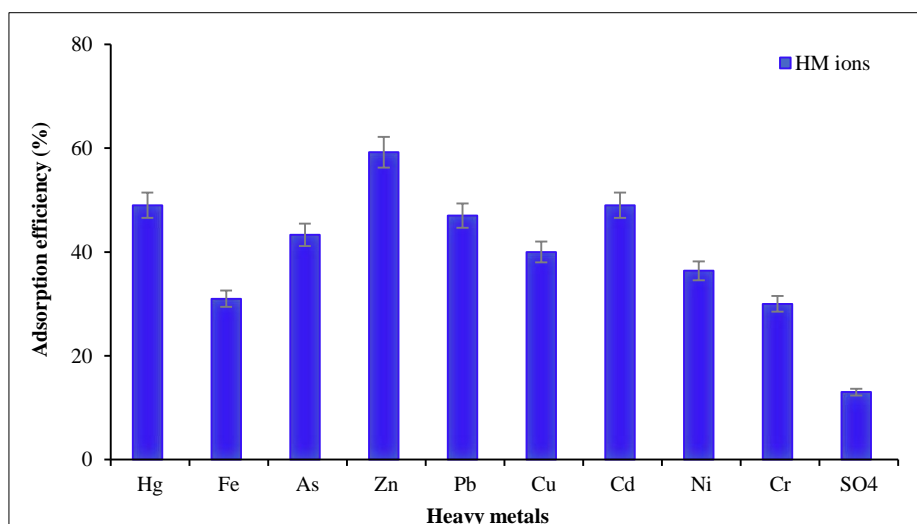


Figure 12. The percentages absorbed HM ions at 2 days interaction period

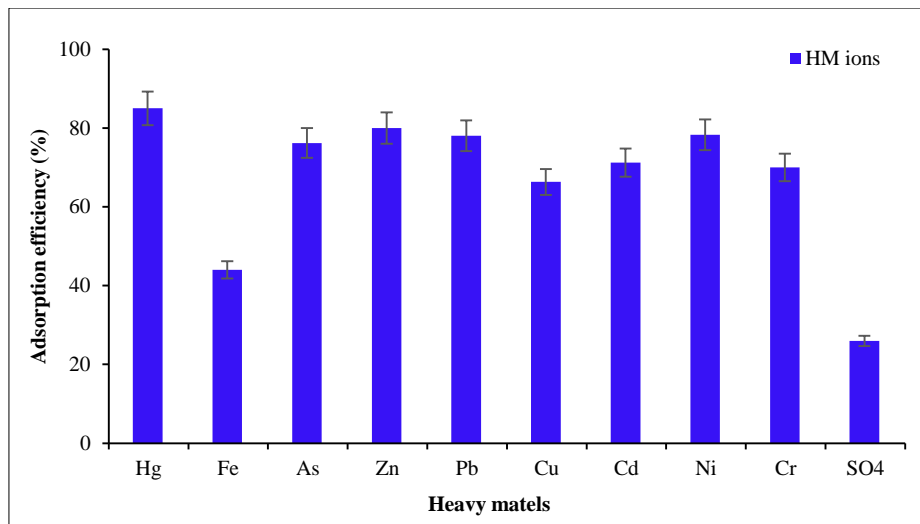


Figure 13. The percentages absorbed HM ions at 5 days interaction period

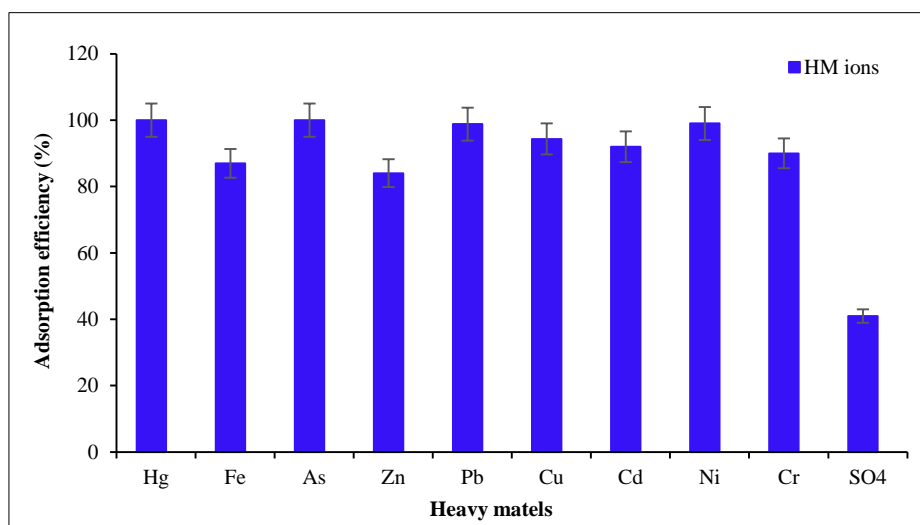


Figure 14. The percentages absorbed HM ions at 7 days interaction period

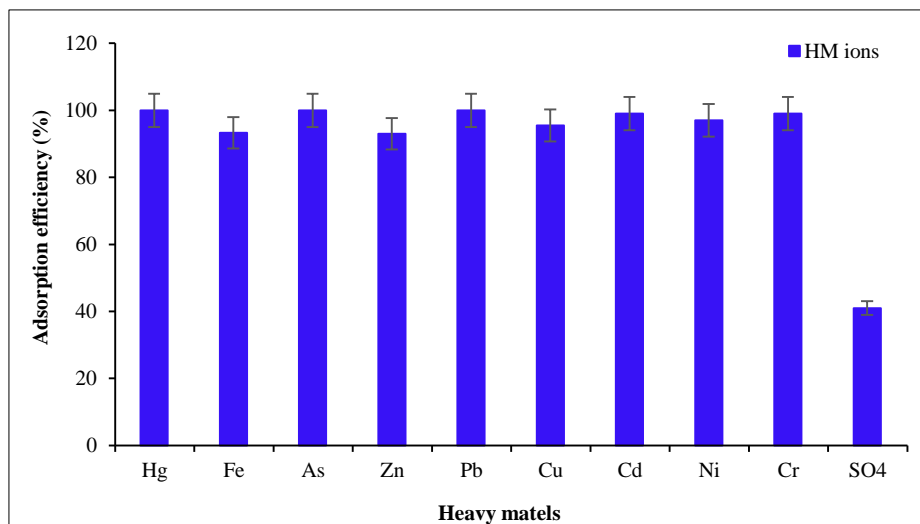


Figure 15. The percentages absorbed HM ions at 10 days interaction period

As was expected significant adsorption percentages of Hg, Fe, Zn, Cu, Ni, and Cr were noted due to the pH, CEC, and charged surface area of the nanomaterial. The results obtained in this study are in line with research work published [53-57]. Their studies concluded that nano-iron was successfully used for the removal of arsenic, whereas graphite oxide at the nanoscale also showed effective uptake of Cr and Pb with a gradual decrease in Ni ion concentration as the dosage of graphene oxide increased [58].

4.5. Scanning Electron Microscopy (SEM) Analysis

The SEM analysis was used to determine the surface morphology of the untreated natural soil liner and NSCL. The microscopy results showed significant physical changes caused by the adsorption of HMs and metalloids after the equilibrium period of 10 days. The SEM analysis traced some gel-like precipitates on the surface of the liners, as shown in Figures 16 to 18. The surface morphology of the liner changes as the dosages of the NBFS increase. This was expected because a higher dosage of NBFS absorbed more HM ions. Therefore, the liner with lesser dosages of NBFS adsorbed fewer HMs, causing the formation of little precipitates on the surface of the liner. However, traces of quartz, pyrophyllite, dicalcium silicate (C₂S), tricalcium silicate (C₃S), calcium silicate hydrate (CSH), calcium aluminate hydrate CAS, and free calcium oxide (f-CaO). Among the mineral precipitates traced at the surface of the liner includes gehlenite (Ca₂Al₂SiO₇), akermanite (Ca₂MgSiO₇), bredigite (Ca₅MgSi₃O₁₂), and merwinite (Ca₃Mg(SiO₄)₂), and gypsum (CaSO₄·2H₂O). The formation of these minerals was expected due to the high sulfate contained in the contaminated water, coupled with the ionic exchange release of OH⁻ and Ca²⁺ from the tertiary precipitates of the reaction.

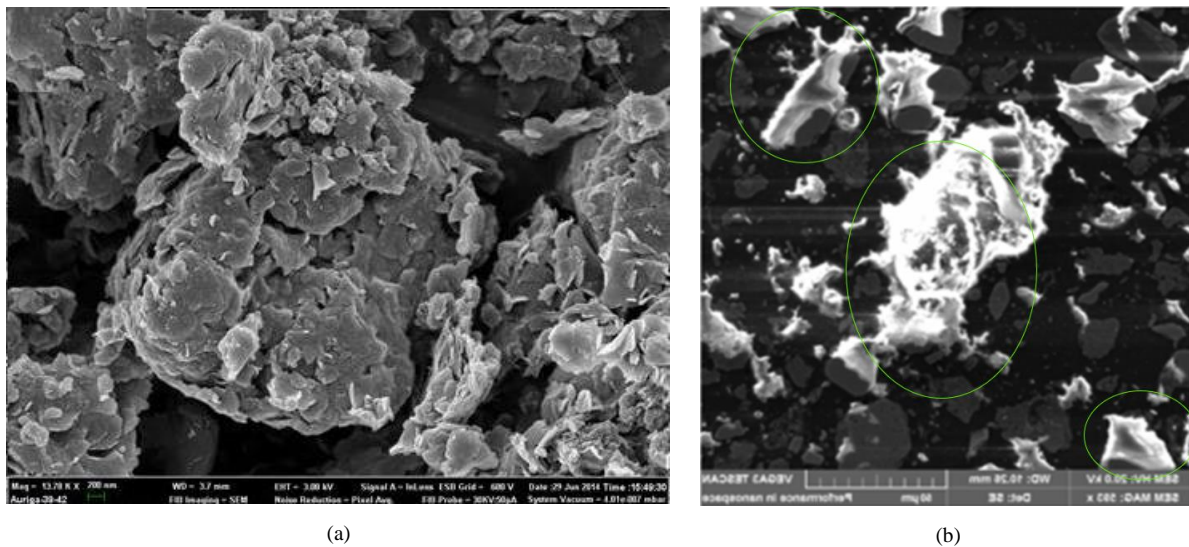


Figure 16. (a) Showing microstructures of natural soil. (b) Showing traces of mineral precipitated formed with 90: 10 ratio of soil and nano-slag

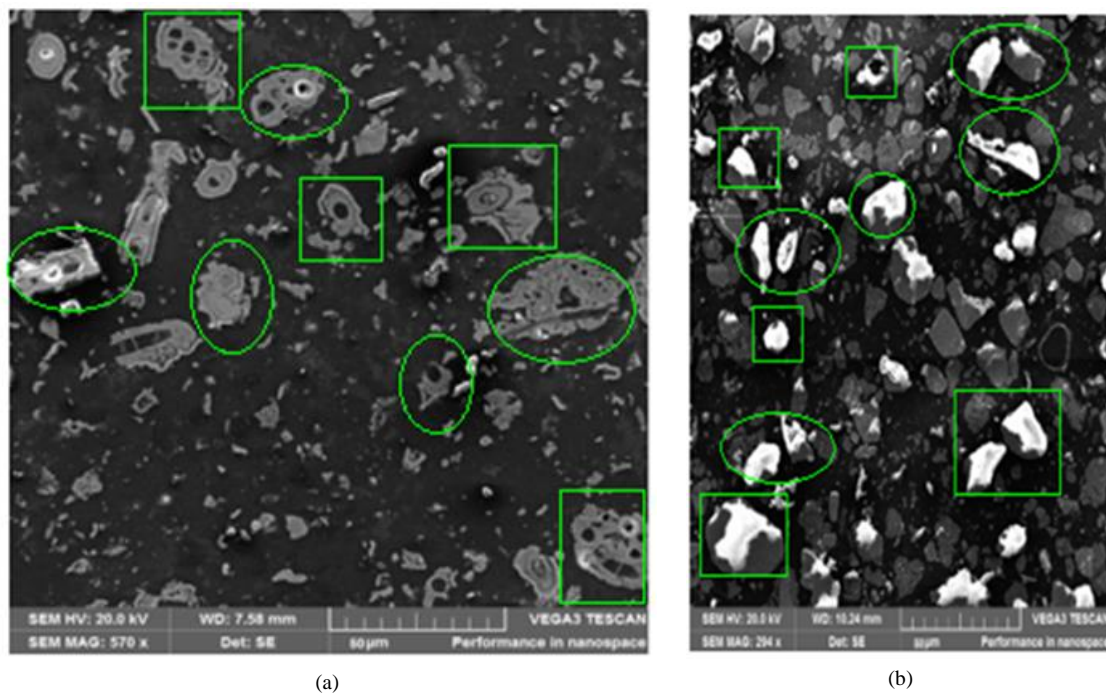


Figure 17. (a) Showing traces of mineral precipitated formed with 80: 20 ratio of soil and NBFS (b) Showing traces of mineral precipitated formed with 70: 30 ratios of soil and nano-slag

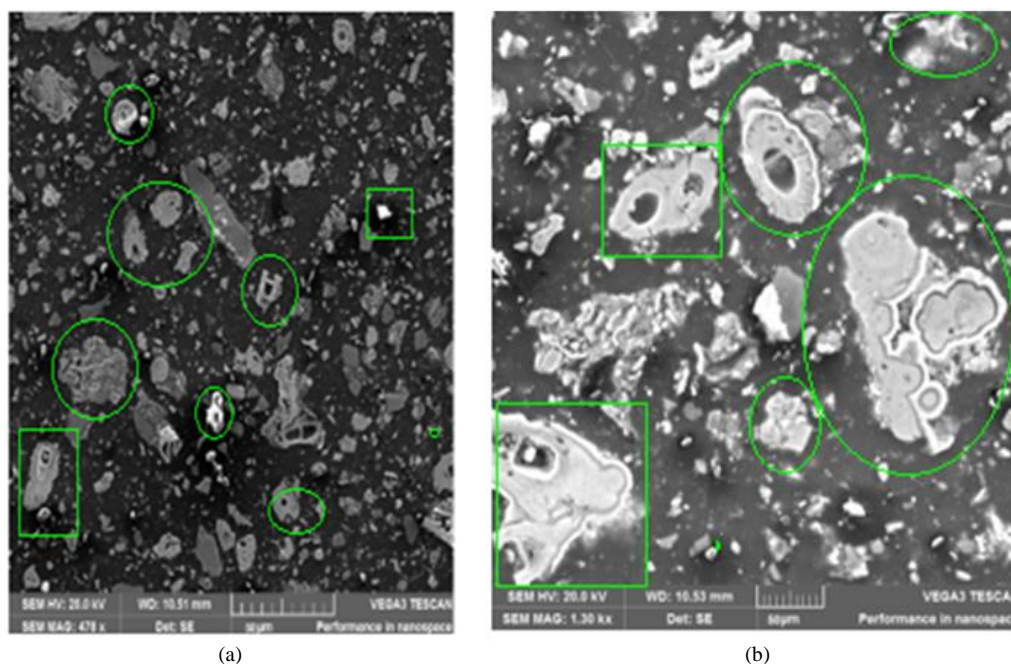


Figure 18. (a) Showing traces of mineral precipitated formed with a 60: 40 ratios of soil and nano-slag (b) Showing traces of mineral precipitated formed with a 50: 50 ratios of soil and nano-slag

In summary, it is observed that nano-slag contains a significant aluminosilicate component, capable of improving sorption rate. Thus, the large surface area of the nano-slag effectively adsorbed the targeted heavy metal ions and metalloids through the combined contribution of ion exchange, precipitation, and ion complexation with heavy metals. The presence of metal oxide, and the nanoparticle size effects, and the elevated temperature produced by the LMT increased the active site on the surface of the liner. The adsorbed HM ions co-precipitated during the pozzolanic reaction and formed gel-like structures with metalloid salts. The concentration of the wastewater before treatment was evaluated to be 2.5 on the pH scale; this implies that the wastewater is toxic due to the presence of metalloids and heavy metals. However, the concentration of the effluents was in the pH range of 7.5 to 7.8, quantifying the effluents fit for livestock, irrigation, and drinking according to DWARF and WHO standards. On the contrary, the natural clay failed to adsorb HM ions due to the liquid-solid partitioning, which is governed by aqueous solubility as a function of pH.

Despite the fact that the nano-slag used in this study has shown significant capacity for adsorbing metalloids, it has a few limitations and drawbacks. The nanomaterials in general are unstable and tend to aggregate, thus reducing their removal capacity of the adsorbent. Furthermore, it is usually difficult to separate the nanomaterials from the aqueous solution swiftly and efficiently due to their nanoscale size. The problems of aggregation, poor separation, and excessive pressure drop when used in fixed-bed and flow-through systems should not be neglected [59].

5. Conclusions

This study evaluates the efficiency of adsorbing HMs (As, Cd, and Pb) using leachate modular tower (LMT) embedded nanomaterial (nano-slag). It is evident that the major challenge of nanomaterials in adsorbing HMs and metalloids is clotting; however, this study proved that increasing the temperature of the interaction between the contaminated water (adsorbate) and nanomaterial (adsorbent) restricted clotting of the system and also improved the rate of sorption at extended interaction times. Based on the obtained results, the removal of 98%As, 99%Cd, and 99.9%Pb was achieved with a 50%:50% ratio of soil and nano-slag as the adsorbent at 10 days equilibrium period. Also, significant adsorption of 98%Zn, 95.45%Cu, 93.3%Fe, 97%Ni, and 89%Hg were achieved upon further study using the same dosage of soil and nano-slag and interaction time. The scanning electron microscopy (SEM) tests revealed that some traces of the absorbed HMs and metalloids were found on the liner surfaces, indicating significant changes in microstructure through precipitation mechanisms. The sorption rate increased significantly due to the elevated temperature, aluminosilicate structure, and prolonged contact time, which are also associated with the elevated pH level and higher cation exchange capacity (CEC) of the liner.

The LMT-embedded nanomaterials exhibit great efficiency in adsorbing heavy metals, as evaluated in this study. Nevertheless, there are still some impediments that need to be addressed to make better use of the LMT embedded nanomaterials for the adsorption of HMs from wastewater. First, the nanoslag used herein tends to aggregate, thus reducing its removal capacity. Furthermore, it is usually difficult to separate the nanomaterials from the aqueous solution swiftly and efficiently due to their nanoscale size. Again, the synthesis process, long-term performance, and some other issues correlated with nanoslag with respect to the developed LMT need to be studied further. Second, the commercial nanoslag used for heavy metal removal on an industry scale is rare, and more efforts are needed to develop market-

available nanomaterials. The synthesis as well as the operating costs of nanoslag should be optimized for the sake of the economy, and the production of nanoslag should meet the requirements of green chemistry. Also, the increasing use of nanoslag in wastewater treatment, their impacts, and their toxicities towards both the environment and human beings should be taken into consideration.

This research produced modified activated carbon from local bamboo using a two-step carbonization and impregnation process. The optimal parameters for the adsorption of heavy metals at different operating conditions in single metal, bimetal, and trimetal solutions were evaluated using Box-Behnken Design (BBD).

This work proposed the study of pH influence on the biosorption process for chromium (Cr⁶⁺), nickel (Ni²⁺), and lead (Pb²⁺) ions in an aqueous solution, searching for a range of pH values ideal to promote the maximum removal rate of these metals under the established conditions. In addition, four lignocellulosic materials were tested as biosorbents: walnut shell (*Carya illinoensis*), chestnut shell (*Castanea sativa*), wood (*Pinus* spp.), and burnt wood (*Pinus* spp.), which are low-cost and easily obtainable agroindustrial wastes. The main objective of this work is to determine an optimal pH that could remove the maximum amount of these three pollutants using low-cost materials available in the region of Viseu, Portugal.

6. Declarations

6.1. Author Contributions

Conceptualization, F.A. and J.A.; methodology, F.A. and J.A.; software, F.A.; validation, F.A. and J.A.; formal analysis, F.A.; investigation, F.A. and J.A.; resources, J.A.; data curation, F.A.; writing—original draft preparation, F.A.; writing—review and editing, J.A.; visualization, F.A.; supervision, F.A. and J.A.; project administration, F.A.; funding acquisition, J.A. All authors have read and agreed to the published version of the manuscript.

6.2. Data Availability Statement

The data presented in this study are available in the article.

6.3. Funding

The authors received financial support from the University of KwaZulu Natal, South Africa, for the publication of this article.

6.4. Acknowledgement

The authors would like to thank the Geotechnics and Materials Development Research Group (GMDRg) and the Water Research Group of the Department of Civil Engineering, University of KwaZulu-Natal, for the support provided for this research.

6.5. Conflicts of Interest

The authors declare no conflict of interest.

7. References

- [1] Briffa, J., Sinagra, E., & Blundell, R. (2020). Heavy metal pollution in the environment and their toxicological effects on humans. *Heliyon*, 6(9). doi:10.1016/j.heliyon.2020.e04691.
- [2] WHO. (2008). Guidelines for drinking-water quality: incorporating 1st and 2nd addenda (3rd Ed.). World Health Organization (WHO), Geneva, Switzerland. Available online: https://apps.who.int/iris/bitstream/handle/10665/204411/9789241547611_eng.pdf?sequence=1&isAllowed=y (accessed on April 2023).
- [3] Bind, A., Kushwaha, A., Devi, G., Goswami, S., Sen, B., & Prakash, V. (2019). Biosorption valorization of floating and submerged macrophytes for heavy-metal removal in a multi-component system. *Applied Water Science*, 9(4), 95. doi:10.1007/s13201-019-0976-y.
- [4] Kumar, M., Goswami, L., Singh, A. K., & Sikandar, M. (2019). Valorization of coal fired-fly ash for potential heavy metal removal from the single and multi-contaminated system. *Heliyon*, 5(10). doi:10.1016/j.heliyon.2019.e02562.
- [5] Kumar, S., Islam, A. R. M. T., Hasanuzzaman, M., Salam, R., Khan, R., & Islam, M. S. (2021). Preliminary assessment of heavy metals in surface water and sediment in Nakuvadra-Rakiraki River, Fiji using indexical and chemometric approaches. *Journal of Environmental Management*, 298. doi:10.1016/j.jenvman.2021.113517.
- [6] Fu, Z. J., Jiang, S. K., Chao, X. Y., Zhang, C. X., Shi, Q., Wang, Z. Y., Liu, M. L., & Sun, S. P. (2022). Removing miscellaneous heavy metals by all-in-one ion exchange-nanofiltration membrane. *Water Research*, 222, 118888. doi:10.1016/j.watres.2022.118888.

- [7] Toropitsyna, J., Jelinek, L., Wilson, R., & Paidar, M. (2023). Selective Removal of Transient Metal Ions from Acid Mine Drainage and the Possibility of Metallic Copper Recovery with Electrolysis. *Solvent Extraction and Ion Exchange*, 41(2), 176–204. doi:10.1080/07366299.2023.2181090.
- [8] Sun, Y., Wang, Z., Chen, J., Fang, Y., Wang, L., Pan, W., Zou, B., Qian, G., & Xu, Y. (2022). Phosphorus Recovery from Incinerated Sewage Sludge Ash Using Electrodialysis Coupled with Plant Extractant Enhancement Technology. *SSRN Electronic Journal*. doi:10.2139/ssrn.4293133.
- [9] Khan, A. U., Khan, A. N., Waris, A., Ilyas, M., & Zamel, D. (2022). Phytoremediation of pollutants from wastewater: A concise review. *Open Life Sciences*, 17(1), 488–496. doi:10.1515/biol-2022-0056.
- [10] Li, Q., Liu, D., Chen, C., Shao, Z., Wang, H., Liu, J., Zhang, Q., & Gadd, G. M. (2019). Experimental and geochemical simulation of nickel carbonate mineral precipitation by carbonate-laden Ureolytic fungal culture supernatants. *Environmental Science: Nano*, 6(6), 1866–1875. doi:10.1039/c9en00385a.
- [11] Rajendran, S., Priya, A. K., Senthil Kumar, P., Hoang, T. K. A., Sekar, K., Chong, K. Y., Khoo, K. S., Ng, H. S., & Show, P. L. (2022). A critical and recent developments on adsorption technique for removal of heavy metals from wastewater-A review. *Chemosphere*, 303(N), 0045–6535,. doi:10.1016/j.chemosphere.2022.135146.
- [12] Lejwoda, P., Świnder, H., & Thomas, M. (2023). Evaluation of the stability of heavy metal-containing sediments obtained in the wastewater treatment processes with the use of various precipitating agents. *Environmental Monitoring and Assessment*, 195(4), 442. doi:10.1007/s10661-023-11036-9.
- [13] Li, Y., Yu, H., Liu, L., & Yu, H. (2021). Application of co-pyrolysis biochar for the adsorption and immobilization of heavy metals in contaminated environmental substrates. *Journal of Hazardous Materials*, 420(126655). doi:10.1016/j.jhazmat.2021.126655.
- [14] Kushwaha, A., Rani, R., & Patra, J. K. (2020). Adsorption kinetics and molecular interactions of lead [Pb(II)] with natural clay and humic acid. *International Journal of Environmental Science and Technology*, 17(3), 1325–1336. doi:10.1007/s13762-019-02411-6.
- [15] Gupta, A., Sharma, V., Sharma, K., Kumar, V., Choudhary, S., Mankotia, P., Kumar, B., Mishra, H., Moulick, A., Ekielski, A., & Mishra, P. K. (2021). A review of adsorbents for heavy metal decontamination: Growing approach to wastewater treatment. *Materials*, 14(16). doi:10.3390/ma14164702.
- [16] Maleki, A., Mohammad, M., Emdadi, Z., Asim, N., Azizi, M., & Safaei, J. (2020). Adsorbent materials based on a geopolymer paste for dye removal from aqueous solutions. *Arabian Journal of Chemistry*, 13(1), 3017–3025. doi:10.1016/j.arabjc.2018.08.011.
- [17] Luhar, I., Luhar, S., Abdullah, M. M. A. B., Razak, R. A., Vizureanu, P., Sandu, A. V., & Matasaru, P. D. (2021). A state-of-the-art review on innovative geopolymer composites designed for water and wastewater treatment. *Materials*, 14(23), 7456. doi:10.3390/ma14237456.
- [18] Aigbe, U. O., & Osibote, O. A. (2020). A review of hexavalent chromium removal from aqueous solutions by sorption technique using nanomaterials. *Journal of Environmental Chemical Engineering*, 8(6), 104503. doi:10.1016/j.jece.2020.104503.
- [19] Bandar, S., Anbia, M., & Salehi, S. (2021). Comparison of MnO₂ modified and unmodified magnetic Fe₃O₄ nanoparticle adsorbents and their potential to remove iron and manganese from aqueous media. *Journal of Alloys and Compounds*, 851. doi:10.1016/j.jallcom.2020.156822.
- [20] Nworie, F. S., Mgbemena, N., Ike-Amadi, A. C., & Eburnoha, J. (2022). Functionalized Biochars for Enhanced Removal of Heavy Metals from Aqueous Solutions: Mechanism and Future Industrial Prospects. *Journal of Human, Earth, and Future*, 3(3), 377-395. doi:10.28991/HEF-2022-03-03-09.
- [21] Xiao, G., Wang, Y., Xu, S., Li, P., Yang, C., Jin, Y., Sun, Q., & Su, H. (2019). Superior adsorption performance of graphitic carbon nitride nanosheets for both cationic and anionic heavy metals from wastewater. *Chinese Journal of Chemical Engineering*, 27(2), 305–313. doi:10.1016/j.cjche.2018.09.028.
- [22] Ibrahim, R. K., Hayyan, M., AlSaadi, M. A., Hayyan, A., & Ibrahim, S. (2016). Environmental application of nanotechnology: air, soil, and water. *Environmental Science and Pollution Research*, 23(14), 13754–13788. doi:10.1007/s11356-016-6457-z.
- [23] Mathur, J., Goswami, P., Gupta, A., Srivastava, S., Minkina, T., Shan, S., & D. Rajput, V. (2022). Nanomaterials for Water Remediation: An Efficient Strategy for Prevention of Metal (Loid) Hazard. *Water (Switzerland)*, 14(24), 3998. doi:10.3390/w14243998.
- [24] Kumara, G. M. P., & Kawamoto, K. (2019). Applicability of crushed clay brick and municipal solid waste slag as low-cost adsorbents to refine high concentrate Cd (II) and Pb (II) contaminated wastewater. *International Journal of Geomate*, 17(63), 133–142. doi:10.21660/2019.63.26726.

- [25] Nguyen, T. C., Tran, T. D. M., Dao, V. B., Vu, Q. T., Nguyen, T. D., & Thai, H. (2020). Using Modified Fly Ash for Removal of Heavy Metal Ions from Aqueous Solution. *Journal of Chemistry*, 2020, 11. doi:10.1155/2020/8428473.
- [26] Praditia, T., Karlbauer, M., Otte, S., Oladyskhin, S., Butz, M. V., & Nowak, W. (2022). Learning Groundwater Contaminant Diffusion-Sorption Processes with a Finite Volume Neural Network. *Water Resources Research*, 58(12), 2022 033149. doi:10.1029/2022WR033149.
- [27] Ahmadi, M., Hazrati Niari, M., & Kakavandi, B. (2017). Development of maghemite nanoparticles supported on cross-linked chitosan (γ -Fe₂O₃@CS) as a recoverable mesoporous magnetic composite for effective heavy metals removal. *Journal of Molecular Liquids*, 248, 184–196. doi:10.1016/j.molliq.2017.10.014.
- [28] Akpomie, K. G., Conradie, J., Adegoke, K. A., Oyedotun, K. O., Ighalo, J. O., Amaku, J. F., Olisah, C., Adeola, A. O., & Iwuozor, K. O. (2023). Adsorption mechanism and modeling of radionuclides and heavy metals onto ZnO nanoparticles: a review. *Applied Water Science*, 13(1). doi:10.1007/s13201-022-01827-9.
- [29] ASTM D1140-17. (2017). Standard Test Methods for Determining the Amount of Material Finer than 75- μ m (No. 200) Sieve in Soils by Washing, ASTM International, Pennsylvania, United States. doi:10.1520/D1140-17.
- [30] IS 2720-24. (1976). Methods of test for soils Part XXIV determination of cation exchange capacity. Bureau of Indian Standards, New Delhi, India.
- [31] South African Water Quality Guidelines. (1976). Volume 7: Aquatic Ecosystems. Department of Water Affairs and Forestry (DWARF), Mokopane, South Africa.
- [32] ASTM D6276-19. (2019). Standard Test Method for Using pH to Estimate the Soil-Lime Proportion Requirement for Soil Stabilization. ASTM International, Pennsylvania, United States. doi:10.1520/D6276-19.
- [33] Dubey, R., Bajpai, J., & Bajpai, A. K. (2016). Chitosan-alginate nanoparticles (CANPs) as potential nanosorbent for removal of Hg (II) ions. *Environmental Nanotechnology, Monitoring and Management*, 6, 32–44. doi:10.1016/j.enmm.2016.06.008.
- [34] Chen, C., Liu, H., Chen, T., Chen, D., & Frost, R. L. (2015). An insight into the removal of Pb(II), Cu(II), Co(II), Cd(II), Zn(II), Ag(I), Hg(I), Cr(VI) by Na(I)-montmorillonite and Ca(II)-montmorillonite. *Applied Clay Science*, 118, 239–247. doi:10.1016/j.clay.2015.09.004.
- [35] Zacaroni, L. M., Magriotis, Z. M., Cardoso, M. das G., Santiago, W. D., Mendonça, J. G., Vieira, S. S., & Nelson, D. L. (2015). Natural clay and commercial activated charcoal: Properties and application for the removal of copper from cachaça. *Food Control*, 47, 536–544. doi:10.1016/j.foodcont.2014.07.035.
- [36] Campillo-Cora, C., Conde-Cid, M., Arias-Estévez, M., Fernández-Calviño, D., & Alonso-Vega, F. (2020). Specific adsorption of heavy metals in soils: Individual and competitive experiments. *Agronomy*, 10(8). doi:10.3390/agronomy10081113.
- [37] Ewis, D., Ba-Abbad, M. M., Benamor, A., & El-Naas, M. H. (2022). Adsorption of organic water pollutants by clays and clay minerals composites: A comprehensive review. *Applied Clay Science*, 229. doi:10.1016/j.clay.2022.106686.
- [38] Kolluru, S. S., Agarwal, S., Sireesha, S., Sreedhar, I., & Kale, S. R. (2021). Heavy metal removal from wastewater using nanomaterials-process and engineering aspects. *Process Safety and Environmental Protection*, 150, 323–355. doi:10.1016/j.psep.2021.04.025.
- [39] Ghasemzadeh, G., Momenpour, M., Omid, F., Hosseini, M. R., Ahani, M., & Barzegari, A. (2014). Applications of nanomaterials in water treatment and environmental remediation. *Frontiers of Environmental Science and Engineering*, 8(4), 471–482. doi:10.1007/s11783-014-0654-0.
- [40] Rajak, A. A. (2022). Emerging technological methods for effective farming by cloud computing and IoT. *Emerg. Sci. J.*, 6(5), 1017-1031. doi:10.28991/ESJ-2022-06-05-07.
- [41] Zarime, N. A., Yaacob, W. Z. W., & Jamil, H. (2018). Removal of heavy metals using bentonite supported nano-zero valent iron particles. *AIP Conference Proceedings*. doi:10.1063/1.5027944.
- [42] Sadegh, H., Ali, G. A. M., Gupta, V. K., Makhlof, A. S. H., Shahryari-ghoshekandi, R., Nadagouda, M. N., Sillanpää, M., & Megiel, E. (2017). The role of nanomaterials as effective adsorbents and their applications in wastewater treatment. *Journal of Nanostructure in Chemistry*, 7(1), 1–14. doi:10.1007/s40097-017-0219-4.
- [43] Sepehri, S., Kanani, E., Abdoli, S., Rajput, V. D., Minkina, T., & Asgari Lajayer, B. (2023). Pb(II) Removal from Aqueous Solutions by Adsorption on Stabilized Zero-Valent Iron Nanoparticles—A Green Approach. *Water (Switzerland)*, 15(2), 222. doi:10.3390/w15020222.
- [44] Alipour, A., Zarinabadi, S., Azimi, A., & Mirzaei, M. (2020). Adsorptive removal of Pb(II) ions from aqueous solutions by thiourea-functionalized magnetic ZnO/nanocellulose composite: Optimization by response surface methodology (RSM). *International Journal of Biological Macromolecules*, 151, 124–135. doi:10.1016/j.ijbiomac.2020.02.109.

- [45] Zhang, Y., Zhang, H., Zhang, Z., Liu, C., Sun, C., Zhang, W., & Marhaba, T. (2018). PH Effect on Heavy Metal Release from a Polluted Sediment. *Journal of Chemistry*, 2018, 7. doi:10.1155/2018/7597640.
- [46] Yu, G., Wang, X., Liu, J., Jiang, P., You, S., Ding, N., Guo, Q., & Lin, F. (2021). Applications of nanomaterials for heavy metal removal from water and soil: A review. *Sustainability (Switzerland)*, 13(2), 1–14. doi:10.3390/su13020713.
- [47] Cruz-Lopes, L. P., Macena, M., Esteves, B., & Guiné, R. P. F. (2021). Ideal pH for the adsorption of metal ions Cr⁶⁺, Ni²⁺, Pb²⁺ in aqueous solution with different adsorbent materials. *Open Agriculture*, 6(1), 115–123. doi:10.1515/opag-2021-0225.
- [48] Huang, J., Yuan, F., Zeng, G., Li, X., Gu, Y., Shi, L., Liu, W., & Shi, Y. (2017). Influence of pH on heavy metal speciation and removal from wastewater using micellar-enhanced ultrafiltration. *Chemosphere*, 173, 199–206. doi:10.1016/j.chemosphere.2016.12.137.
- [49] Zafar, M. N., Aslam, I., Nadeem, R., Munir, S., Rana, U. A., & Khan, S. U. D. (2015). Characterization of chemically modified biosorbents from rice bran for biosorption of Ni(II). *Journal of the Taiwan Institute of Chemical Engineers*, 46, 82–88. doi:10.1016/j.jtice.2014.08.034.
- [50] Zafar, M. N., Saeed, M., Nadeem, R., Sumra, S. H., Shafiqat, S. S., & Qayyum, M. A. (2019). Chemical pretreatments of *Trapa bispinosa*'s peel (TBP) biosorbent to enhance adsorption capacity for Pb(II). *Open Chemistry*, 17(1), 325–336. doi:10.1515/chem-2019-0031.
- [51] Penha, R. S., Santos, C. C., Cardoso, J. J. F., Silva, H. A. S., Santana, S. A. A., & Bezerra, C. W. B. (2016). Chemically treated rice husk as low-cost adsorbent for metal ions uptake (Co²⁺ and Ni²⁺). *Revista Virtual de Quimica*, 8(3), 588–604. doi:10.5935/1984-6835.20160045.
- [52] Yadav, N., Singh, S., Saini, O., & Srivastava, S. (2022). Technological advancement in the remediation of heavy metals employing engineered nanoparticles: A step towards cleaner water process. *Environmental Nanotechnology, Monitoring and Management*, 18, 100757. doi:10.1016/j.enmm.2022.100757.
- [53] Tang, X., Zheng, H., Teng, H., Sun, Y., Guo, J., Xie, W., Yang, Q., & Chen, W. (2016). Chemical coagulation process for the removal of heavy metals from water: a review. *Desalination and Water Treatment*, 57(4), 1733–1748. doi:10.1080/19443994.2014.977959.
- [54] Kołodyńska, D., Krukowska-Bąk, J., Kazmierczak-Razna, J., & Pietrzak, R. (2017). Uptake of heavy metal ions from aqueous solutions by sorbents obtained from the spent ion exchange resins. *Microporous and Mesoporous Materials*, 244, 127–136. doi:10.1016/j.micromeso.2017.02.040.
- [55] Yang, J., Hou, B., Wang, J., Tian, B., Bi, J., Wang, N., Li, X., & Huang, X. (2019). Nanomaterials for the Removal of Heavy Metals from Wastewater. *Nanomaterials*, 9(3), 424. doi:10.3390/nano9030424.
- [56] Jaishankar, M., Tseten, T., Anbalagan, N., Mathew, B. B., & Beeregowda, K. N. (2014). Toxicity, mechanism and health effects of some heavy metals. *Interdisciplinary Toxicology*, 7(2), 60–72. doi:10.2478/intox-2014-0009.
- [57] Xu, J., Cao, Z., Zhang, Y., Yuan, Z., Lou, Z., Xu, X., & Wang, X. (2018). A review of functionalized carbon nanotubes and graphene for heavy metal adsorption from water: Preparation, application, and mechanism. *Chemosphere*, 195, 351–364. doi:10.1016/j.chemosphere.2017.12.061.
- [58] Gopalakrishnan, A., Krishnan, R., Thangavel, S., Venugopal, G., & Kim, S. J. (2015). Removal of heavy metal ions from pharma-effluents using graphene-oxide nanosorbents and study of their adsorption kinetics. *Journal of Industrial and Engineering Chemistry*, 30, 14–19. doi:10.1016/j.jiec.2015.06.005.
- [59] Hua, M., Zhang, S., Pan, B., Zhang, W., Lv, L., & Zhang, Q. (2012). Heavy metal removal from water/wastewater by nanosized metal oxides: A review. *Journal of Hazardous Materials*, 211–212, 317–331. doi:10.1016/j.jhazmat.2011.10.016.